



Synthesis of Expanded Graphite : Effect of the graphite flake size on adsorption capacities to Methylene Blue

Hoang Thi Chien, Vu Thi Huong Ly, Tran Thi Thao, Vu Thi Thuy, Nguyen Thi Ngan, Nguyen Hai Thanh, Vu T. Tan*

School of Chemical Engineering, Hanoi University of Science and Technology, Hanoi, VIETNAM

*Email: tan.vuthi@hust.edu.vn

Hội thảo "Khoa học và Công nghệ Hóa vô cơ lần thứ V" - Hà Nội 2021

ARTICLE INFO

Received: 15/2/2021

Accepted: 15/5/2021

Published: 30/6/2021

Keywords:

Expanded Graphite,
 Adsorption, Flake size,
 Methylene Blue

ABSTRACT

For the first time, the expansion grade of graphite was studied through the effect of the flake size. The result shown the larger flake size exhibits a higher expansion grade. In addition, the more expanded material, the higher specific surface area can be obtained. The synthesized expanded graphites were used for the adsorption of methylene blue. The expanded graphite with the highest expansion grade displayed the highest adsorption capacity due to its specific surface area.

Introduction

The dye pollutants from several industrial sources, such as paper, pharmaceutical, plastics, paint, or textile industries, are harmful to the environment and very dangerous to humans [1]. The cleaning processes of the dye pollutants play an essential role in environmental sustainability. Recently, various treatment approaches such as chemical oxidation [3], adsorption [3], biological treatment [4], or photocatalyst [5] have been employed to remove the harmful organic dye pollutants from industrial wastewater. Among all the approaches, adsorption is a promising technology for eliminating contaminants due to its low cost, recyclability, high efficiency, and ease of manipulation [6].

Expanded graphite (EG) has gained much attention due to its excellent properties, such as low density, multi-porosity, large-specific surface area, and hydrophobic properties [7]. Recently, EG has been considered essential for adsorption with a high sorption efficiency, especially organic compounds. The

traditional method for the fabrication of EG is the use of graphite intercalation compounds (GICs). GICs are complex graphite materials containing acid molecules and alkali metals, such as Na-THF, K-THF, Co-THF, H₂SO₄, HClO₄ and HNO₃. The EG can be obtained by thermal treatment of GICs at high temperatures [8]. However, the thermal treatment can realize toxic gases and require a high cost, complicated equipment for EG fabrication [9].

For the first time in this work, we reported a simple methodology for the fabrication of EG at room temperature. We also studied the effect of the lateral flake on the expansion grade of Graphite. Besides, this study also compares the adsorption capacity of EG obtained by different lateral flake size on methylene blue adsorption. The results may demonstrate that the expansion of Graphite with the different lateral sizes is a key topic and leads to acquiring a higher EG adsorption capacity.

Experimental

The fabrication of EG

Natural graphite (NG) was collected from Bao Ha mining, Lao Cai province in Vietnam, with a carbon content \geq of 80%. The impurities of NG was removed by HCl 20% for several cycles. The cleaned NG has a carbon content $>$ 97%.

Firstly, a mixture containing 3 g $(\text{NH}_4)_2\text{S}_2\text{O}_8$ and 3 mL concentrated H_2SO_4 (98%) with the weight ratio of 1:2 was mechanically mixed for 5 min. After that, 1g of NG was gradually added into the prepared mixture and stirred for the 60s at room temperature; a slurry comprised of $(\text{NH}_4)_2\text{S}_2\text{O}_8$, H_2SO_4 and NG is obtained. After that, the slurry was translated into a glass vessel with an open cap for the completed expansion. After several hours, the expanded graphite (EG) is neutralized by deionized water to pH neutral.

The expansion process of EG is illustrated in the following scheme.

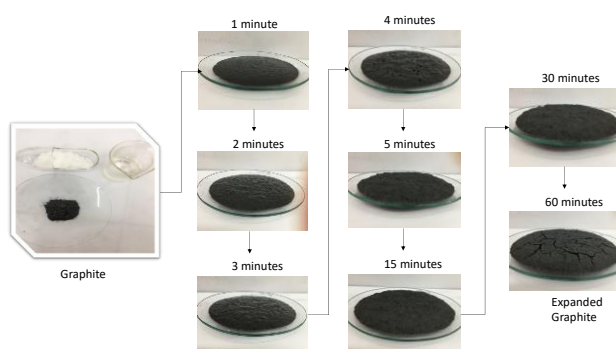


Figure 1: Scheme of the expansion process of Graphite

The final products are denoted according to the lateral size of the graphite initial: EG synthesized from NG with 75 μm is EG-75; EG synthesized from NG with 125 μm is EG-125; EG synthesized from NG with 315 μm is EG-315)

Material characterization

The X-ray diffraction (XRD) patterns of the sample were recorded on a Bruker D8 Advance instrument operating at 40 kV and 40 mA using Cu K α radiation ($\lambda = 0,15406$ nm). The structures and morphology of the samples were studied by scanning electron microscopy (SEM, FEI Quanta FEG 650 model) .the specific surface area of the samples estimated by the Brunauer – Emmett–Teller (BET) equation, the analysis was carried out on a Micromeritics ASAP 2020 analyzer. The Raman spectra were recorded on a micro-Raman spectrophotometer (JASCO Raman NRS-3000) using a 633 nm excited laser at room temperature.

Bath adsorption test

A solution of Methylene Blue (MB) of concentration 20 mg/L was prepared before the adsorption test.

The adsorption process was carried out in the dark to avoid the decomposition of MB by daylight during the adsorption test. A typical experiment was carried out by using a determined amount of adsorbents in the powder form (EG-75; EG-125; EG-315) with 500 mL of standard solution MB. The mixture was stirred during several time intervals to avoid the flotation effect of EG. After the adsorption process, the adsorbents were separated from the liquid by centrifugation at high speed up to 6000 rpm. The concentration of MB in solution was evaluated by using a spectroquant Colorimeter Move 100.

The removal efficiency of the adsorbents was evaluated by the following equation:

$$\text{Removal (\%)} = 100 * (C_0 - C_e) / C_0 \quad (1)$$

where C_0 and C_e are the initial and equilibrium concentrations of MB (mg/L).

Results and discussion

The expansion degree of the three EG samples

The expansion degree of the expanded graphite is determined by the expansion coefficient (K_v). Therefore, the coefficient K_v is chosen as the parameter to evaluate the expansion degree and select the best condition for EG synthesis. The K_v is determined as follows: weigh 0.2 g EG and poured the EG into a 50 mL cylinder (diameter 20 mm). Then the cylinder is gently shaken to deposited the material homogenously. The volume (VEG) of the material is noted according to the occupied volume of the cylinder.

The expansion coefficients of EG-75; EG-125; EG-315 samples are presented in the following table:

Table 1: The expansion degree of the EG-75; EG-125; EG-315 samples

Sample	Expansion coefficient, K_v
EG-75	54.4
EG-125	73.4
EG-315	82.45

The expansion coefficient (K_v) is calculated using the following formula:

$$K_v = V_t / V_0 \quad (2)$$

In which: V_t is the density of the material after the expansion process (mL / g); V_0 is the initial density of Graphite (1.6 mL / g).

From the results presented in Table 1, it can be seen that the larger lateral size (EG-315) displays a higher expansion coefficient.

Chemical and structural characterization of EG

Figure 2 shows the XRD patterns of the NG with the size 315 μm (NG-315), EG-75; EG-125; EG-315 samples. A (002) diffraction peak can be clearly observed on all of the XRD patterns. The (002) XRD pattern of natural graphite shows reflections in the perpendicular direction (c-axis) of the graphite hexagonal planes. However, the (002) diffraction signal of the three EG is much weaker compared to that of the original NG. This result indicates the positional disorder in all EG during the exfoliation of the graphite layers [10].

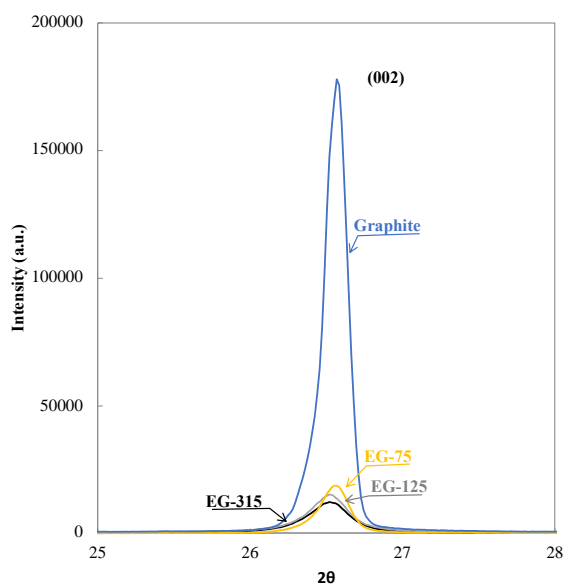


Figure 2: XRD spectra of NG-315, EG-75; EG-125; EG-315

Figure 3 shows that the morphology of NG presents a flat surface with a multilayered crystalline structure. After the process, the interlayer structure of the NG flakes was broadened with different expansion degrees, as found in Figure 2(b–d). The EG-75 presents the smallest distance between two Graphite layers. Meanwhile, the EG-315 reveals a most considerable distance between two Graphene layers. Generally, many packed layers and wrinkles structure, furrows

appear on the surface of the EG-125 and EG-315. In addition, the three EG samples were found in worm-like images with an inner porous structure, which facilitates the transport of dye effluents.

The Raman spectra of NG-315, EG-75; EG-125; EG-315 are shown in Figure 4. Comparatively, the D peak of the three EG samples becomes a little more obvious. And the calculated ratio I_D/I_G is 0, 0.42; 0.50; 0.65 corresponded to NG, EG-75; EG-125; EG-315, respectively.

The ratio $I_D/I_G > 0$ indicating the structural disordering of the material. In this work, The EG-315 presents the highest I_D/I_G , which indicates the most disordering of the material after the expansion process. Thus, the result shows that the EG-315 is more expanded comparing with the smaller lateral size. The results are well in agreement with the calculation of expansion degree, XRD, SEM, and BET results.

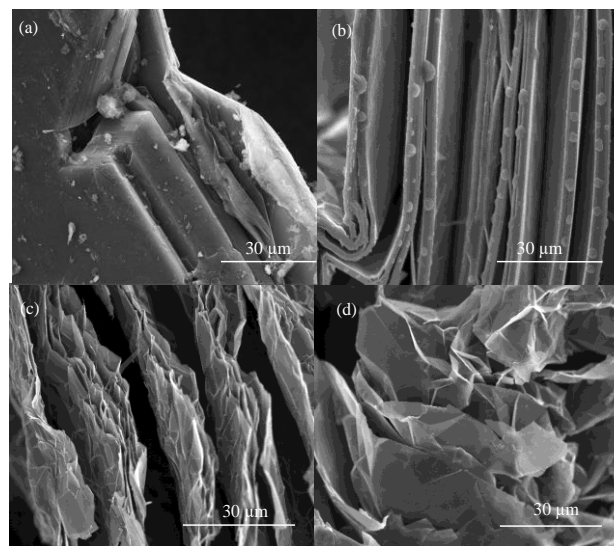


Figure 3: SEM images of NG-315 (a), EG-75 (b), EG-125 (c) and EG-315 (d)

The characterization of the specific surface area of the adsorbents plays an essential part in the MB adsorption capacity. Table 1 exhibits the specific surface area of NG, EG-75; EG-125; EG-315 samples. The results show that EG-315 shows the highest specific surface area. This result can be explained by its expansion degree.

All the characterization results demonstrated that the expansion degree of EG depends on the lateral size of graphite. This is the first study focused on the relation between the expansion degree of EG and graphite lateral size. In our opinion, the H_2SO_4 is challenging to penetrate the graphite flake when the lateral size is small. This makes the expansion degree is lower compared with the large lateral size.

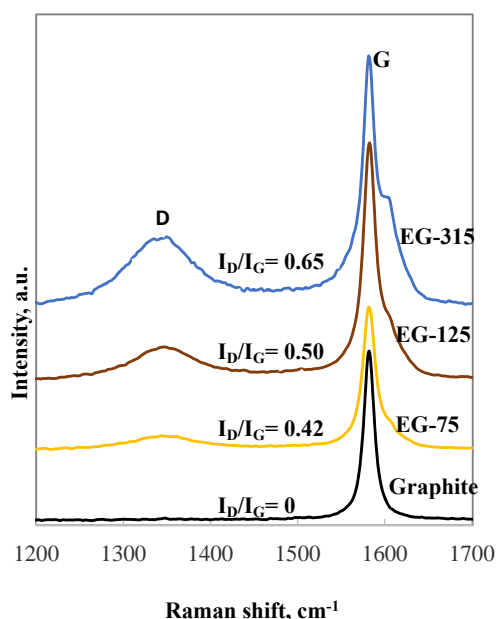


Figure 4: Raman spectra of NG-315, EG-75, EG-125, EG-315

Table 2: The specific surface area of the material

Sample	Specific surface area, m ² /g
NG-315	5.21
EG-75	8.31
EG-125	18.03
EG-315	20.04

Adsorption capacity of the expanded graphite

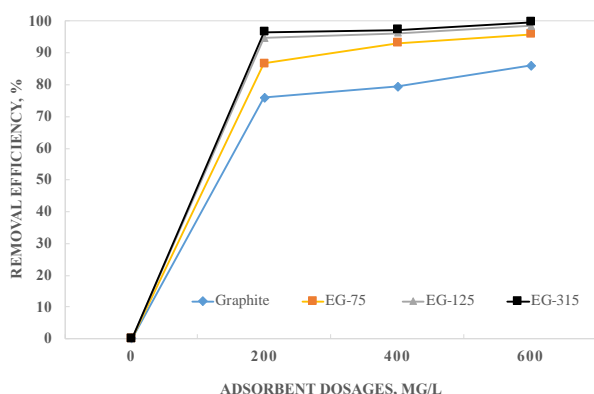


Figure 5: The removal efficiency of the adsorbent

It is already known that the adsorbent dosage affects the adsorption capacity of methylene blue [11]. In this

work, the effect of adsorbent dosage was studied at an initial dye concentration of 20 mg/l, pH of 5, and contact time of 60 minutes. The adsorbent dosages are varied from 0 to 600 mg/L. Figure 4 shows that the removal efficiency is improved with an increase in the adsorbent dosage of all the materials NG-315, EG-75; EG-125; EG-315. The results may relate to the rise in the active sites on the surface of the adsorbents due to the higher concentration of adsorbent [12].

It can be seen that the EG-315 exhibits the highest adsorption efficiency on MB comparing with the NG-315 or EG-75, EG-125. This result can be explained by the specific surface area of the EG-315. Therefore, the adsorption capacity of the expanded graphite is strongly dependent on the lateral size of the initial graphite. The larger the lateral size, the higher the adsorption capacity can be obtained.

Conclusion

In this study, several samples of expanded graphite with different lateral sizes were produced at low temperatures. The expansion degree of Graphite is intensely determined by the lateral size of the initial Graphite. The result showed that the larger the lateral size, the expansion degree of the material is higher. The adsorption capacities of all the materials were tested on MB adsorption. The EG-315 shown higher adsorption capacity than the other EG (EG-75 and EG-125).

The chemical and structure characterizations of the obtained samples show that expanded graphite can be achieved at low temperatures. The results open a new chance for the fabrication of high-quality, expanded graphite as an adsorbent for the organic dye pollutant treatment.

Acknowledgments

This research is funded by Vietnam Ministry of Education and Training under grant number B2020-BKA-562-22.

References

1. T. T. Vu, L. del Río, T. Valdés-Solís, and G. Marbán, J. Hazard. Mater., 246-247(2013) 126-134. <https://doi.org/10.1016/j.jhazmat.2012.12.009>.
2. S. H. Lin and S. J. Ho, Waste Manage., 17(1997) 71-78. [https://doi.org/10.1016/S0956-053X\(97\)00039-1](https://doi.org/10.1016/S0956-053X(97)00039-1).

3. J. Qu, *J. Environ. Sci.*, 20(2008) 1-13. [https://10.1016/S1001-0742\(08\)60001-7](https://10.1016/S1001-0742(08)60001-7).
4. J. L. Sanz and T. Köchling, *Process Biochem.*, 42(2007) 119-133. <https://10.1016/j.procbio.2006.10.003>.
5. M. N. Chong, B. Jin, C. W. K. Chow, and C. Saint, *Water Res.* 44(2010) 2997-3027. <https://10.1016/j.watres.2010.02.039>.
6. J. Akhtar, N. A. S. Amin, and K. Shahzad, *Desal. Water Treat.* 57(2016) 12842-12860. 10.1080/19443994.2015.1051121.
7. S. Tan, P. Shi, R. Su, and M. Zhu, *Adv. Mater. Res.*, 424-425 (2012) 1313-1317. <https://10.4028/www.scientific.net/AMR.424-425.1313>.
8. R. Goudarzi and G. Hashemi Motlagh, *Heliyon* 5(2019) 10. <https://10.1016/j.heliyon.2019.e02595>.
9. M. Salvatore, G. Carotenuto, S. De Nicola, C. Camerlingo, V. Ambrogi and C. Carfagna, *Nano. Res. Lett.* 12(2017) 167. <https://10.1186/s11671-017-1930-2>.
10. E. Falcao, R. Blair, J. Mack, L. Viculis, *Carbon* 45(2007) 1367-1369. <https://10.1016/j.carbon.2007.01.018>.
11. Y. C. Sharma and Uma, *J. Chem. Eng. Data* 55(2010) 435-439. <https://10.1021/je900408s>.
12. H. Shi, W. Li, L. Zhong, and C. Xu, *Ind. Eng. Chem. Res.* 53(2014) 3 1108-1118. <https://pubs.acs.org/doi/abs/10.1021/ie4027154>.